

# Ray Tracing Simulations of ECR Heating and ECE Diagnostic at W7-X Stellarator

Nikolai B. Marushchenko, Volker Erckmann, Hans J. Hartfuss, Mattias Hirsch, Heinrich P. Laqua, Henning Maassberg and Yuri Turkin

## 1 DESCRIPTION OF THE CODE TRAVIS

TRAVIS (TRAsing VISualised): the new powerful ray tracing code. Covers both heating (ECRH/ECCD) and ECE diagnostic.

Idea: to take into account the thermal and non-thermal effects.

- An especially designed graphical user interface: the preparation of input parameters and viewing results in 2D and 3D form.
- 3D magnetic configuration: VMEC → JMC → the mesh stored for rapid interpolation by a specially developed package.
- The ray tracing equations are the standard Hamiltonian ones,

$$\frac{d\mathbf{r}}{ds} = \frac{\partial \mathcal{H}}{\partial \mathbf{k}} \bigg|_{\partial \mathbf{k}}, \quad \frac{d\mathbf{k}}{ds} = -\frac{\partial \mathcal{H}}{\partial \mathbf{r}} \bigg|_{\partial \mathbf{k}}. \quad (1)$$

- Generally, different models for the Hamiltonian can be used:

$$\mathcal{H} = \begin{cases} \mathcal{H}^W = N^2 - N_{\parallel}^2 - (\Re N_{\perp})^2, & \text{model of Westerhof [1],} \\ \mathcal{H}^T = \Re(D_{ij}^H e_i^* e_j), & \text{model of Tokman [2],} \\ \mathcal{H}^s = \Re(\det D_{ij}^H), & \text{standard model,} \end{cases}$$

where  $D_{ij} \equiv N^2 \delta_{ij} - N_i N_j - \epsilon_{ij}$ , and  $e_i$  is the polarization vector.

- The dielectric tensor for tracing is:

$$\epsilon_{ij} = \begin{cases} \epsilon_{ij}^H(\omega, \mathbf{k}) + \epsilon_{ij}^{aH}(\omega, \mathbf{k}), & \text{weakly relativistic: quasiperp. launch,} \\ \epsilon_{ij}^H(\omega, \mathbf{k}) + \epsilon_{ij}^{aH}(\omega, \mathbf{k}), & \text{non relativistic: oblique launch; EBW,} \\ \epsilon_{ij}^H(\omega), & \text{cold: along high } \nabla B. \end{cases}$$

- Absorption and emissivity (see, e.g. [3]),

$$\alpha = \frac{\omega}{4\pi} \frac{\epsilon_{ij}^{aH} E_i^* E_j}{|\mathbf{F}|}, \quad \eta = \pi N_r^2 \frac{\omega^2}{c^2} \frac{G_{ij} E_i^* E_j}{|\mathbf{F}|}, \quad \text{with } \mathbf{F} = -\frac{\omega}{8\pi} \frac{\partial}{\partial \mathbf{k}} (\epsilon_{ij}^H E_i^* E_j),$$

are calculated for an arbitrary electron distribution function,  $f_e$ ,

$$\epsilon_{ij}^{aH} = -\pi \frac{\omega^2}{\omega^2} \sum_n \int d\mathbf{p} p_{\perp} \Pi_{in}^* \Pi_{jn} \delta \left( \gamma - \frac{n\omega_c}{\omega} - \frac{N_{\parallel} p_{\parallel}}{mc} \right) \hat{L} f_e$$

$$G_{ij} = \frac{\pi}{(2\pi)^5} \frac{\omega^2}{\omega^2} \sum_n \int d\mathbf{p} \frac{p_{\perp}^2}{\gamma} \Pi_{in}^* \Pi_{jn} \delta \left( \gamma - \frac{n\omega_c}{\omega} - \frac{N_{\parallel} p_{\parallel}}{mc} \right) f_e$$

In the code,  $f_e$  can be Maxwellian, bi-Maxwellian or numerically given.

- By analysing the value of the magnetic moment, the cyclotron interaction is modelled separately for passing and trapped electrons [4].
- To calculate the CD efficiency the adjoint approach is applied [5, 6].
- ECE spectrum: special options are included to estimate the limit of the spatial resolution and to identify the energy range of emitting electrons [4, 7].

## References

- [1] E. Westerhof, Proc. of the 13th Joint Workshop on EC and ECH, Nizhny Novgorod, Russia, 17-20 May 2004, pp. 15-29
- [2] M.D. Tokman *et al*, Plasma Phys. Control. Fusion 42 (2000) 91
- [3] M. Bornatici *et al*, Nucl. Fusion 23 (1983) 1153
- [4] N.B. Marushchenko *et al*, Fusion Sci. Technol., 50 (2006), 395
- [5] M. Taguchi, Plasma Phys. Control. Fusion 31 (1989) 241
- [6] M. Romé *et al*, Plasma Phys. Control. Fusion 40 (1998) 511
- [7] V. Tribaldos and B.P. van Milligen, Nucl. Fusion 36 (1996) 283

## 2 O2-SCENARIO, HIGH-FIELD-SIDE LAUNCH

Example for W7-X (to demonstrate a flexibility of the device): quasi-perpendicular HFS launch of O2-mode near the “triangular” plane.

Parameters:  $B_0 \equiv \langle B \rangle_{\text{axis}} = 2.59 \text{ T}$ ,  $n_e(0) = 1.5 \cdot 10^{20} \text{ m}^{-3}$ , and  $T_e(0) = 3 \text{ keV}$ . Plasma is “optically gray”, and the power shine-trough is about 17% (Fig.1, right).

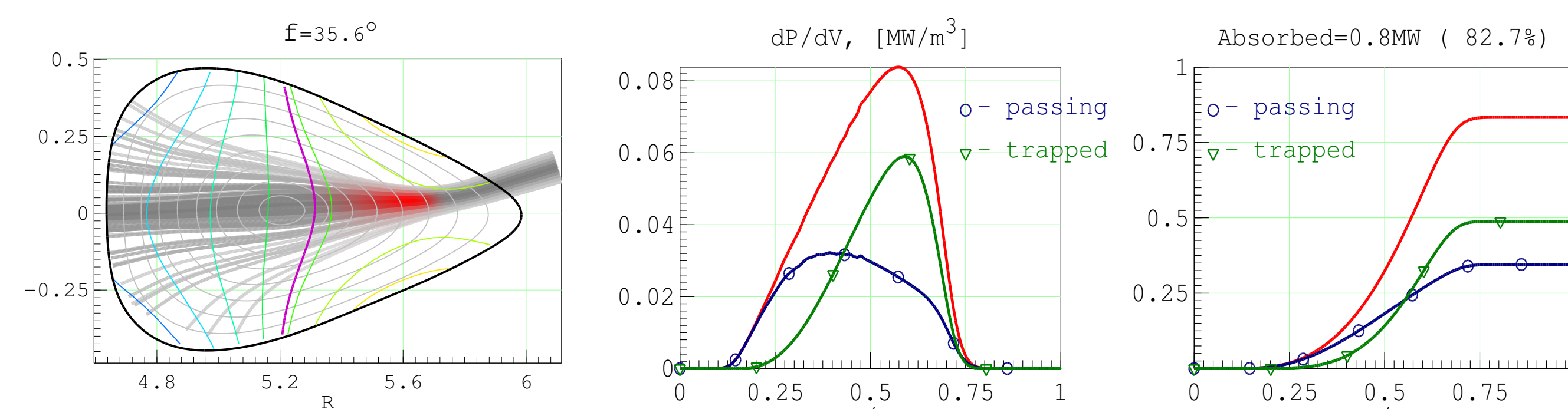


Figure 1. Left: ray trajectories of the O2-mode in the “triangular plane”. The line  $\omega = 2\omega_{ce}$  ( $B=2.5 \text{ T}$ ) is also shown. Middle: deposition profiles for both trapped and passing electrons and the total one. Right: integral absorbed powers.

The most important results:

- about 60% of power is absorbed by ripple trapped electrons (Fig.1, right);
- the shapes of the deposition profiles for trapped and passing electrons are quite different (Fig.1, middle).

Explanation: HFS launch + plasma is optically gray.

- Damping starts from  $r_{\text{eff}}/a \simeq 0.7$ , where  $v/v_{th} \sim 3 \rightarrow$  trapped electrons absorb.
- In  $r_{\text{eff}}/a < 0.4$   $v/v_{th} \sim 1.5$  and  $\tau \sim 1 - 1.5$ , absorption is due to passing electrons.

Opposite example is the X2-mode for  $B_0 = 2.68 \text{ T}$  and  $n_e(0) = 0.5 \cdot 10^{20} \text{ m}^{-3}$  (Fig.1a):

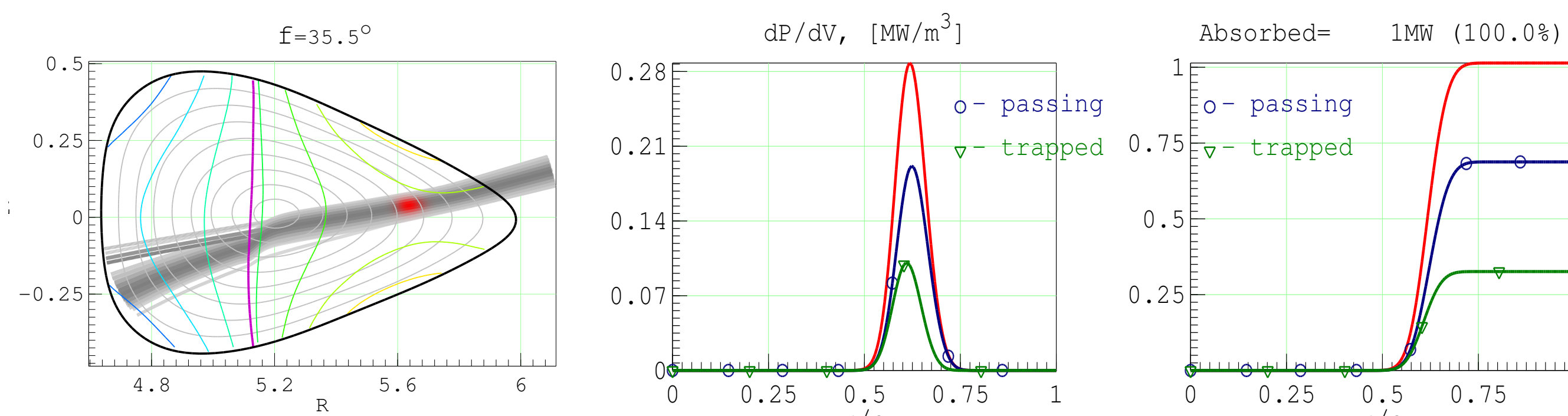


Figure 1a. The same as in Fig.1 for X2-mode.

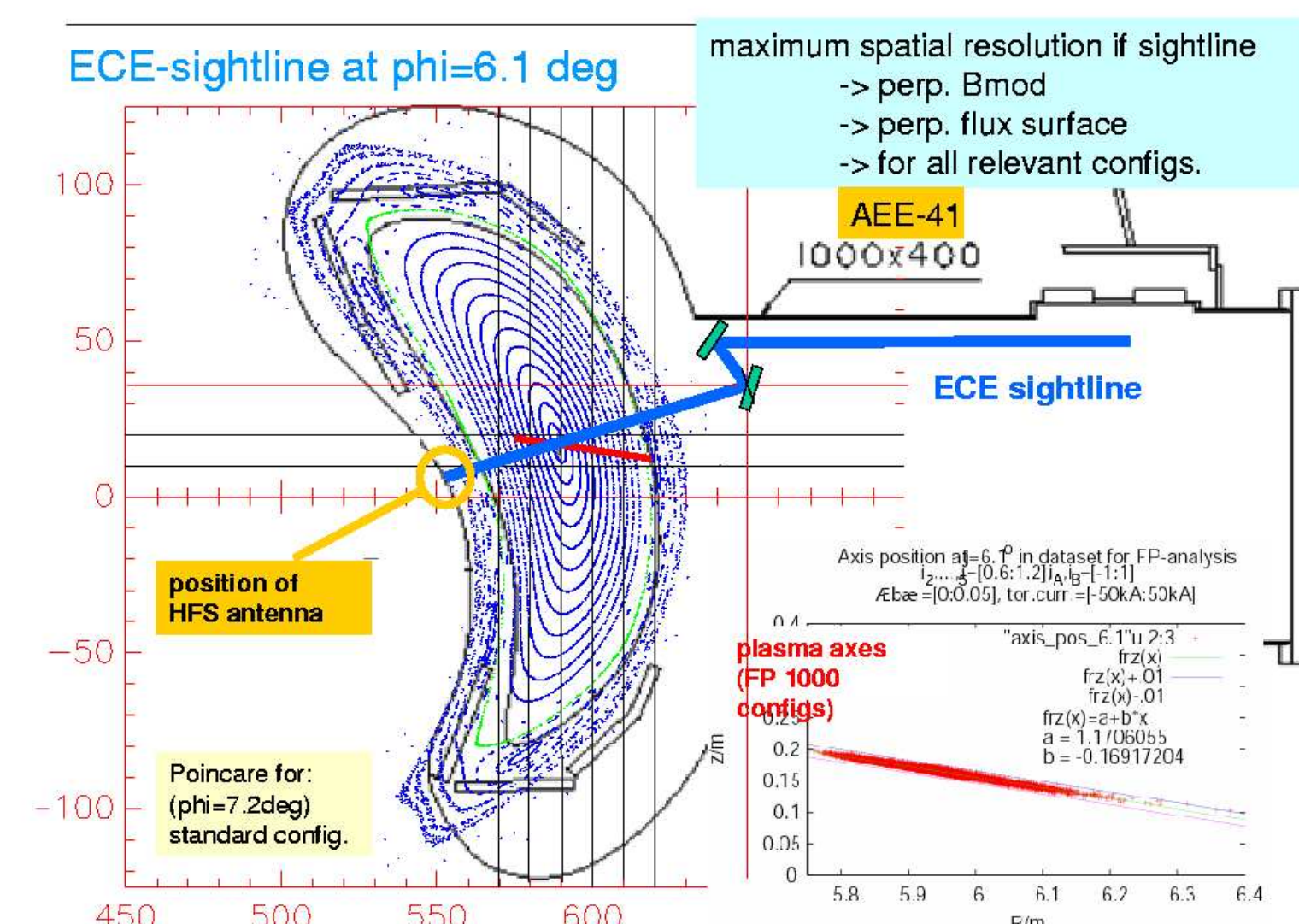
- plasma is optically thick and the conditions in damping region are almost unchanged.

Fraction of trapped particles in the “triangular” plane can be varied in configuration scans. This adds to the flexibility of the launcher.

## 3 ECE DIAGNOSTIC: LFS vs HFS OBSERVATIONS

To illustrate the possibility to distinguish the non-thermal ECE, the results of simulations for both HFS and LFS observations, which are considered for the W7-X ECE diagnostic, are shown and discussed.

- Parameters:  $n_e(0) = 2 \cdot 10^{19} \text{ m}^{-3}$ ,  $T_e(0) = 5 \text{ keV}$ ,  $B_0 = 2.4 \text{ T}$ .
- The port for the LFS antenna is situated close to the “bean-shaped” plane.
- The HFS antenna is assumed to be located at the opposite position.
- The frequency range:
  - 127 GHz  $\leq f \leq$  157 GHz - 2nd harmonic,
  - 180 GHz  $\leq f \leq$  220 GHz - 3rd harmonic range



Electron distribution function is bi-Maxwellian,  $f_e = (1 - \delta)f_{M0} + \delta f_{M1}$

It is assumed, that supra-thermal fraction exists only in the central region,  $r_{\text{eff}} \lesssim 5 \text{ cm}$ , with  $\delta = 0.05$  and  $T_{e1}(0)/T_{e0}(0) = 3$

The results of simulation are shown in Fig.3.

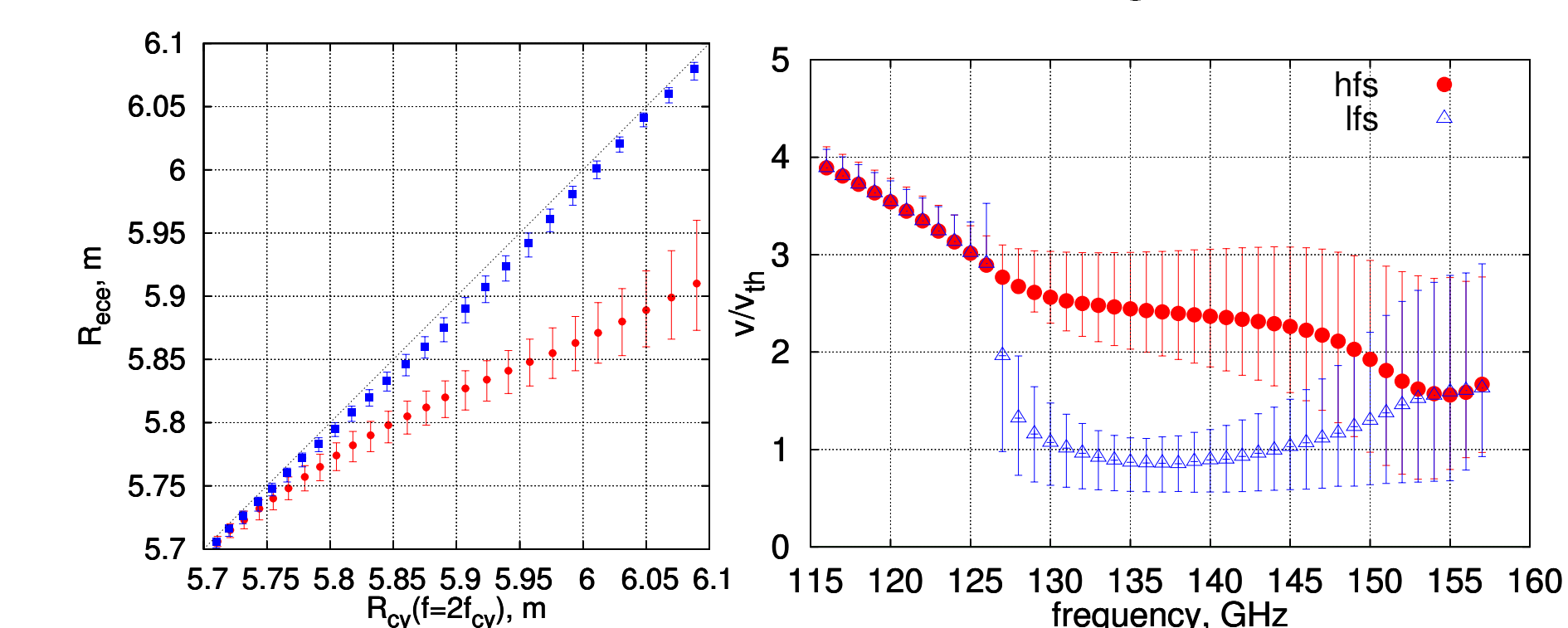


Figure 3. Left: the emission line centers vs the resonance positions for the LFS ( $\Delta$ ) and the HFS ( $\circ$ ) cases. Right: velocity ranges of emitting electrons ( $v_{th}^2 = 2T_e/m$ ).

- LFS: the emission line locations are very close to the “cold” resonance, and the spatial resolution is sufficient (about 5%).
- HFS: the (down-shifted) emission lines are far from the “cold” resonance.
- The resolution for HFS is not as high in comparison with the LFS case.

The HFS emission contains the information about the non-thermal electrons, and being complementary to the LFS one, provide a tool to estimate the weight of the non-Maxwellian fraction.

## 4 SUMMARY

- TRAVIS is a powerful code which covers a broad area of problems in both heating (ECRH/ECCD) and ECE diagnostic
- The code is benchmarked against the old W7-AS code, the code WR\_RTC, the code TORBEAM; succesful test was performed on the ITER reference “Scenario-2”
- Thanks to a general model of the Hamiltonian, the kinetic effects which lead to anomalous dispersion are taken into account.
- Absorption and emissivity can be calculated for arbitrary  $f_e$ .
- Macroscopic quantities such as the deposition profile or the radiative temperature can be decomposed in the contribution from trapped and passing particles.
- The energy range of absorbing and emitting electrons is also calculated.
- The spatial width of the emission line, calculated together with the ECE spectrum, gives the theoretical limit to the spatial resolution of the ECE diagnostic.